

# High-temperature layered composite with a metal matrix, reinforced with single-crystal sapphire fibers

Valery Korzhov, Vyacheslav Kiiko, Vladimir Kurlov  
Institute of Solid State Physics RAS, Chernogolovka, Moscow Region, Russia

**Abstract:** Heat-resistant composites with a layered niobium-based matrix reinforced with single-crystal sapphire fibers have been obtained. The fibers were grown from the melt by the modified Stepanov method. The composites were prepared by solid-phase technology by diffusion welding of multilayer packages of foils of the Nb–0.1% C and aluminum alloy, interlaid with sapphire fibers in layers of a suspension mixture of Nb powder. The production of fibers, their structure and strength testing procedure are described. The formation of multilayer packets, the structure and results of bending strength tests of composites are presented.

**KEYWORDS:** COMPOSITE, LAYERED-FIBROUS STRUCTURE, METAL MATRIX, NIOBIUM, MOLYBDENUM, SAPPHIRE FIBERS, STEPANOV'S METHOD, HEAT RESISTANCE, ULTIMATE STRENGTH, FRACTURE SURFACE.

## 1. Introduction

The development and research of composites with refractory metal matrices is a promising direction, first of all, because it opens up opportunities to increase the operating temperatures of structural elements used in modern engines, including gas turbine ones. This implies an increase in the efficiency of power plants by increasing their efficiency, saving fuel and reducing the burden on the environment. The metal matrix makes the developed composite materials related to metal alloys. It can absorb their advantages, proven by many years of practice, associated, first of all, with the high fracture toughness of many alloys, inaccessible to intermetallic and ceramic materials.

But the possibilities of traditional alloys are practically exhausted today. This is determined either by the limitation of the operating temperature ceiling due to the proximity of the melting temperatures of alloys, for example, based on nickel, leading to low creep resistance [1, 2], or low crack resistance of heavily alloyed alloys, for example, based on niobium [3], or difficulties production and use of refractory structural materials based on, for example, molybdenum due to high density [4], as well as problems associated with gas corrosion [5]. The last two factors apply especially to the materials for the rotor blades of gas turbine engines.

Optimally "designed" composite structures based on a sufficiently plastic matrix reinforced with high-strength (albeit brittle) oxide fibers can provide not only acceptable fracture toughness, but also high strength in a wide temperature range and the required creep resistance at high temperatures. The growing requirements for increasing the ceiling of the working temperatures of structural materials inevitably lead to the need to include traditionally unused compounds (oxides, intermetallic compounds) as essential structural components in their composition. With potentially high stiffness, strength and creep resistance, these joints are brittle in many cases. This poses the challenge of developing non-fragile structures containing fragile components. On the whole, the achievement of a balance in a certain sense of the conflicting requirements of strength, crack resistance and creep resistance is an important problem in the development of this type of materials [2].

The flow of publications on high-temperature materials is practically limitless. But we will note only a few characteristic and related publications related to fibrous and layered composites. It was shown in [6] that the reinforcement of a well-known nickel alloy with eutectic fibers from aluminum oxides and rare earth elements made it possible to obtain the alloy creep resistance of 150 MPa at 1150°C and 1% deformation in 100 hours. An example of a layered composite based on niobium and titanium with an operating temperature of up to 1200°C for use in moderately loaded structural elements is presented in [7]. We also note recent works [8–10] aimed at obtaining composites for temperatures up to 1400°C with oxide and silicide fibers and a molybdenum matrix.

But we are not aware of any publications on high-temperature laminated composites reinforced with oxide fibers using solid-phase technology for their production. In this sense, the presented work is new. In it, for the first time, composites with a multilayer matrix based on niobium or niobium, molybdenum and aluminum are

strengthened by reinforcing the matrices with high-strength single-crystal sapphire fibers obtained by the Stepanov method.

The experimental data presented in this work open up, in fact, a new direction in the development and research of composites of this kind, which combine high-strength oxide fibers and a crack-resistant, potentially creep-resistant layered composite matrix containing high-temperature alloys, solid solutions, and intermetallic compounds in a hierarchically organized structure. The presented materials are the results and development of the work carried out by the authors on the development and study of high-temperature layered and layered-fibrous composites [11–14].

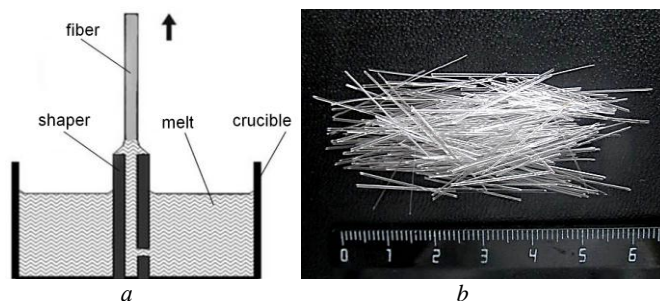
The composites developed in this work not only realize the advantages of high-strength reinforcing oxide fibers and crack-resistant layered composite matrices with strong intermetallic and plastic metal solid solutions contained in them, but also the advantages of specially organized boundaries between structural components that inhibit crack propagation [15]. They allow themselves to still achieve higher characteristics due to the synergistic effect of optimally organized structures [16], which can significantly exceed the characteristics estimated by the "rule of mixtures".

A method for producing fibers, their structure and test procedure for strength, structure, and results of testing fiber-reinforced composites for bending strength are presented. In addition, the presence of relatively light oxide fibers and intermetallic layers in these structures reduce the density of the materials compared to the base metals on the basis of which the materials are made. This increases the specific mechanical characteristics of composites in general, which is very important for many applications.

## 2. Production and testing of single crystal sapphire fibers

Sapphire fibers 150–300 μm in diameter were grown from the melt by the modified Stepanov / EFG (Edge-defined Film-fed Growth) method [17] (Fig. 1, a).

The fibers were formed from a melt of aluminum oxide Al<sub>2</sub>O<sub>3</sub> filling a molybdenum crucible with a shaper containing a capillary channel. The melt rose to the top and was then pulled into the cold zone by a single crystal sapphire seed. The pulling speed was 200–300 mm/h. The resulting fibers were up to one and a half meters long.



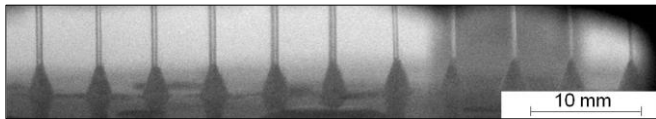


**Fig. 1.** Scheme of obtaining sapphire fibers from a melt, the arrow shows the direction of fiber pulling (a), a bundle of fibers prepared for reinforcing composite prototypes (b) and a scheme of group fiber growth (c)

A group growing method was used (Fig. 1, c), which made it possible to significantly increase the productivity of fiber production. This method is beneficial to the real use of fibers not only as a reinforcing component in structural composite materials, but also in other areas of their application. A bundle of fibers prepared for reinforcing experimental composites 35 mm wide is shown in Fig. 1, b.

The strength of the fibers was determined by the method [18], which consisted in winding individual fibers, previously fixed on an adhesive tape, around rigid cylinders (Fig. 2, a), which consistently differed in diameters from maximum to minimum. In the process of winding, the fibers were broken (Fig. 2, b).

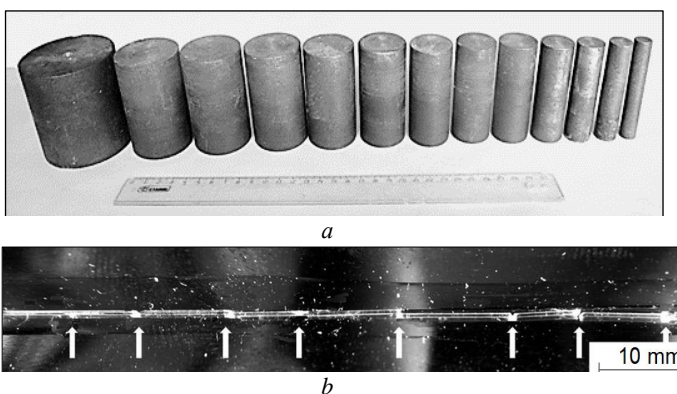


**Fig. 2.** Cylinders used when testing fibers for bending (a) and fiber after testing (b): arrows indicate the points of fracture

At each diameter, the maximum fracture strain arising in the fiber was determined  $\varepsilon = d/D$  (d is the fiber diameter, D is the cylinder diameter) and the average distance between fractures. As a result, a dependence of the breaking deformation of the fiber  $\varepsilon$  on its length was obtained (Fig. 3, a: each character corresponds to one fiber). Taking into account the brittle fracture with a linear nature of the deformation behavior of the material, multiplying the values of  $\varepsilon$  by Young's modulus E, taken for sapphire, equal to 400 GPa, we obtain the dependence of the fiber strength on its length.

The test results showed a rather high strength of the fibers, which was facilitated by their developed fracture surface (Fig. 3, b). Such fracture surfaces of fibers located in the structure of metal composites are capable of initiating micro fracture clouds in the adjacent matrix in the zone of their breakage. This increases the fracture toughness of the composite structure as a whole.

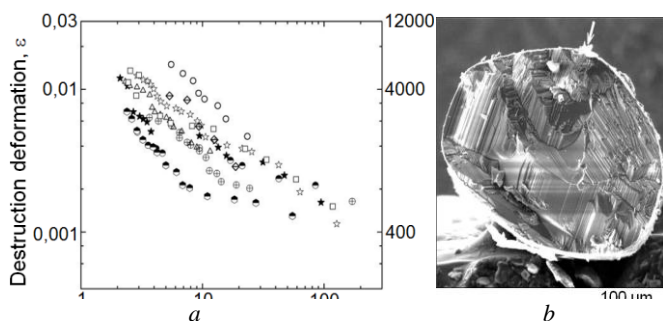


**Fig. 3.** Results of bending tests of fibers: dependence of ultimate deformation at break and strength of fibers on their length (a) and fracture surface of one of the tested fibers, the arrow shows the direction of load application during tests (b)

Stepanov's method used to obtain fibers was improved by a system for stabilizing the diameter of grown fibers [19] (Fig. 4, a), developed at our institute. With the help of it, the vibrations of the fibers that appeared in the ascending gas flow of the thermal zone of the installation for growing crystals were removed.

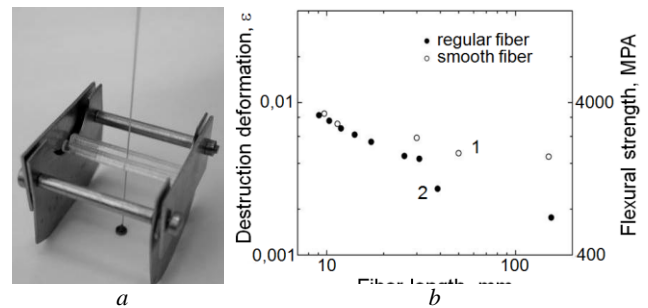


**Fig. 4.** Device for stabilizing the position of the fiber during their growth (a) and the dependence of the ultimate deformation and bending strength of the fiber grown with stabilizing device 1 and without device 2 (b) on the fiber length

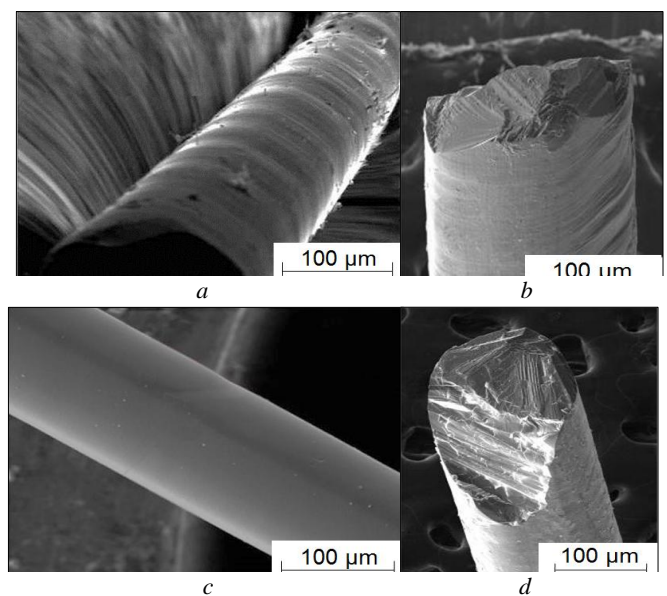


**Fig. 5.** Surfaces (a and c) and sections of fiber breaks after tests (b and d) grown in the usual way (a and b) and with a device for stabilization (c and d)

Mechanical tests showed that fibers grown with a stabilizing device had a higher strength, starting from a length of 20 mm and more (Fig. 4, b). Stabilization of fiber growth removed the roughness of their surface, which significantly increased its optical transmission. In addition, a smooth fiber almost always had an oblique fracture, which significantly exceeded the area of the fracture of rough fibers, which passed across the fiber (Fig. 5, b and d).

### 3. Obtaining, structure and results of strength tests of composites reinforced with sapphire fibers

The basic elements of the layered composite with a niobium matrix were a U-shaped element made of Nb-0.1%C alloy foil 0.25 mm thick and a U-shaped element 1 (see Fig. 6) made of Al-foil 10  $\mu$ m thick, containing one row of sapphire fibers in a finely dispersed Nb-powder of technical purity.

The production of aluminum U-cells 1 was carried out in this way. The counted number of sapphire fibers was laid out with a given pitch and parallel to each other on one of the inner Al surfaces along the width of the U-element and fixed with glue. Then the layer of fibers was "poured" with a suspension coating on polyvinyl-butyril made of commercially pure niobium powder, which dries at room temperature. It was better if the coating thickness was slightly greater than the fiber diameter. This layer

was covered from above with the other half of the Al element (see Fig. 6).

In fig. 6 shows an assembly diagram of the main elements of a composite with an Nb matrix.

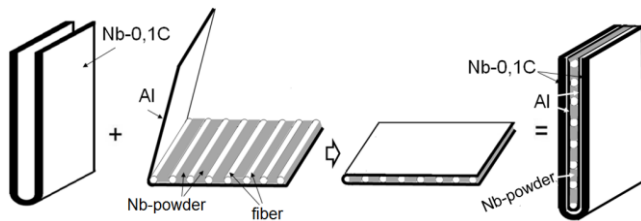


**Fig. 6.** Manufacturing of initial U-elements (1 and 2) for a multilayer package based on niobium: U-element made of Nb-0.1% C alloy foil; 1 – U-element made of Al-foil with sapphire fibers and Nb-powder; 2 – U-element from Nb-0.1% C + U-element 1

It was expected that the layer of "commercially pure Nb-powder" will largely determine the strength, stiffness and creep resistance of the entire composite.

The total number of Al-foil U-elements in the composite is 9 pcs., five of them are enclosed inside the U-shaped foil of the Nb-0.1% C alloy, forming element 2 (see Fig. 6). Four other elements 1 are placed between elements 2 at the final assembly of the package.

Thus, the initial package for obtaining a layered composite based on an Nb-0.1% C alloy reinforced with sapphire fibers was assembled from elements 1 and 2 in the amount of four and five pieces, respectively (Fig. 7, a). The length and width of both elements, and then the dimensions of the package, were ~60 and ~30 mm, respectively. The length of the fibers used varied from 25 to 28 mm, the average diameter was 0.3 mm. Note that the fibers were laid along the element width, which coincided with the direction of rolling of the Nb-C alloy foils.

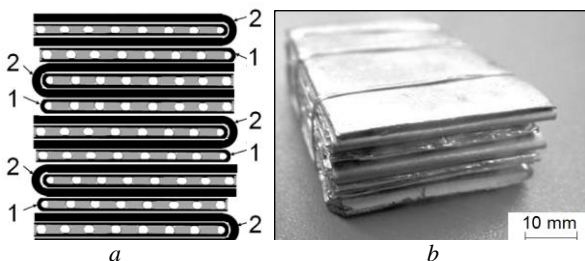


**Fig. 7.** Schematic drawing of a longitudinal section of a multilayer package assembly (a) and a really formed package with segments of TEG tapes on surfaces (b): 1 – U-elements from Al-foil with Nb-powder and sapphire fibers, 2 – U-elements from alloy Nb-0.1% C with U-elements 1 inside

Of interest was also the total length of consumed sapphire fibers in 9 layers with 65 segments in each layer, if their average length was 26.5 mm. Then the total number of used segments is 585, and the total length of the entire sapphire fiber spent on assembling the multilayer package was 15.7 m.

We also note the following. The purpose of the Al-foils in the package is wider than being a container for sapphire fibers. The melting point of aluminum, equal to 660°C, promotes the initial bonding of the components of the welded package, which have significantly higher melting points. As for the contacting Al/Nb pair in the composite, the result of their interpenetration was the formation of intermetallic compounds NbAl<sub>3</sub> (already at 550–600°C) and much higher-temperature Nb<sub>2</sub>Al and Nb<sub>3</sub>Al, stable up to 1800°C and higher, and, therefore, capable to some extent determine the strength, crack resistance, elastic modulus, and creep resistance of the matrix, and, therefore, the entire composite.

In fig. 7, b shows an experimental package composed of elements 1 and 2 in the amount of 4 and 5 pieces, respectively. Both

outer surfaces of the package are covered with two ribbons of thermally expanded graphite (TEG) 0.3 mm thick.

In this form, the package was subjected to solid-phase sintering under pressure P in a diffusion welding installation equipped with a high-strength graphite heater in a vacuum of ~10<sup>-4</sup> Hg. Art. by mode: 1400°C at 12 MPa for 30 min (Fig. 8). The package 1 was located between the movable and stationary punches 3. Between them and the package were laid two pieces of TEG tape, which prevented the package from possible welding to the surface of the punches. Heating to the melting point of aluminum was carried out in a slow (~ 1.5 h) mode so that aluminum, before reaching its melting point, could form an intermetallic compound NbAl<sub>3</sub> with niobium with a high (1680°C) melting point.

After diffusion welding (DW) at 1400°C, the thickness of the package was ~3 mm (Fig. 9). A reflection of the package design is the macrostructure of the cross-section of the laminated composite after welding (Fig. 10), which is an alternation of layers of a light background made of Nb-C alloy and layers of sintered Nb powder with sapphire fibers. The volume fraction of sapphire fibers in the composite was 18%.

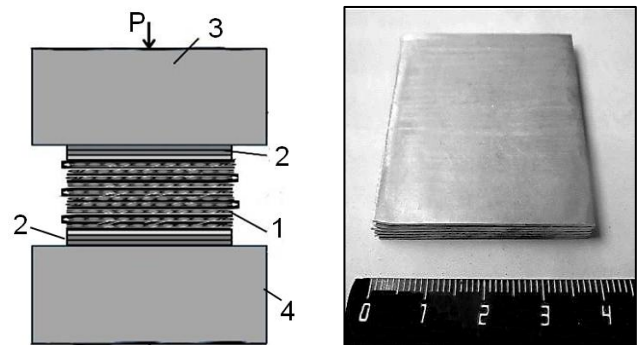


**Fig. 8.** Location of the multilayer package in the diffusion welding installation: 1 – package; 2 – gasket of two TEG strips; 3, 4 – upper and lower punches, P – pressure

**Fig. 9.** Package after diffusion welding

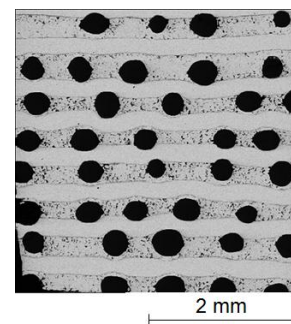


**Fig. 10.** Macrostructure of a layered composite based on niobium after DW

After solid-phase sintering, the package was subjected to heat treatment (HT) in a vacuum resistance furnace according to the mode: 1750°C, 2 h at 0.16 MPa + 1950°C, 2 h at 0.28 MPa. A slight pressure was created due to the fact that the package was "under the yoke" of the Mo-load. The microstructure of the composite in the state "after HT" is shown in Fig. 11.

The structure and phase composition of the composites were studied using Tescan VEGA-II XMU and CamScan MV230 digital scanning electron microscopes (VEGA TS 5130MM). Microscopes are equipped with detectors of secondary and reflected electrons and energy-dispersive X-ray microanalyzers. Microscopes are equipped with detectors of secondary and reflected electrons and energy-dispersive X-ray microanalyzers. The probe size is 5–7 μm.

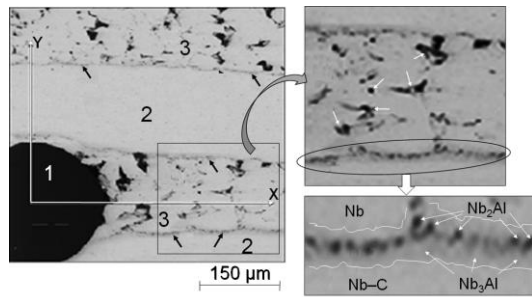


**Fig. 11.** Microstructure of the longitudinal (along the length) section of the composite based on niobium after DW + HT: 1 – sapphire fiber; 2 – a layer of foil made of an Nb-0.1%C alloy; 3 – a layer of Nb powder.

It can be stated that the layered structure of the composite had a lapidary character and consisted of layers 2 that inherited the foils of the Nb-C alloy and layers 3 that inherited the powder coating and, therefore, contained many pores ranging in size from <math>\lt;1\text{ to }20\text{--}25\ \mu\text{m}</math>. In the microstructure fragment outside the main microstructure, the pores are shown by short arrows and are surrounded by a light halo.

The boundaries between sapphire fibers 1 and both matrix layers 2 and 3 appear to be clear, especially if they fall on the Nb-C alloy foil. The complete non-interaction of sapphire with the matrix layer of sintered Nb powder is evidenced by the concentration dependences of Nb and Al along the X axis (Fig. 12, a), plotted from the data of local X-ray spectral (XS) analysis.

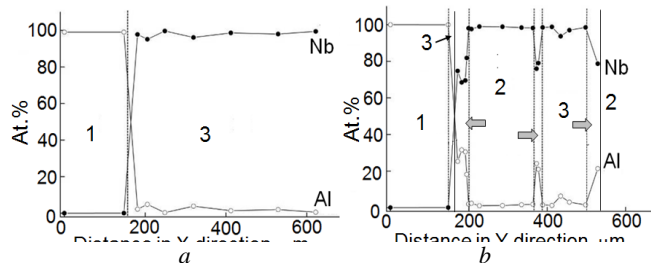


**Fig. 12.** Concentration dependences of Nb (●) and Al (○) according to local RS analysis along the X (a) and Y (b) axes: 1 – sapphire fiber; 2 and 3 – layers inheriting foils of Nb-C alloy and Nb-powder, respectively; horizontal markers show layers of Nb<sub>2</sub>Al and Nb<sub>3</sub>Al

The boundaries between the foils made of the Nb-C alloy and the powder component of the niobium composite were of interest for the study. In a multilayer bag, they were separated by an Al foil. After DW and HT, thin interlayers with a thickness of no more than 1.5  $\mu\text{m}$  were formed in the multilayer composite in place of the Al foils, which did not have clear boundaries, but differed from the neighboring layers by a light gray contrast. In the main figure, they are marked with black arrows. A part of one of the interlayers is taken out as a separate fragment down-to the right of the figure (see Fig. 11), so that the phase structure of the interlayers also appears. Diffuse inclusions with a contrast from dark gray to black were clearly defined on a light gray background.

Now, after such, in general, simple technical operations with an electron microscopic image, we will be guided by the data of local PC analysis. The concentration dependences in Fig. 12, b showed that these interlayers contain from 20 to 30 at. % Al and the rest is niobium. In the Nb-Al phase diagram, such concentrations correspond to the 2-phase region of the intermetallic compounds Nb<sub>3</sub>Al and Nb<sub>2</sub>Al, which are responsible for the colors of gray and dark contrasts, respectively.

Note that, in contrast to the X direction, the first layer in the Y direction after the sapphire is a thin layer of powder niobium 3 (see Figs. 11 and 12, b).

It can be predicted that further holding at high temperatures will form a thin layer of the Nb<sub>3</sub>Al intermetallic compound.

#### 4. Results of the first bending strength tests of composites

After diffusion welding and heat treatment, the composites were in the form of plates ~40 и 50–60 mm and a thickness of 2–2.5 mm (see Fig. 9). Samples for mechanical testing were cut along the width of the bags, that is, along the reinforcing sapphire fibers.

The first 3-point flexural strength tests were carried out at room temperature. The load was applied perpendicular to the layers of the composite. In fig. 13 shows the dependences of the deflection on the load for composites, respectively: after 30-minute diffusion welding under pressure at 1400°C (a) and after welding and two heat treatments at 1750 and 1950°C for 2 h (b).

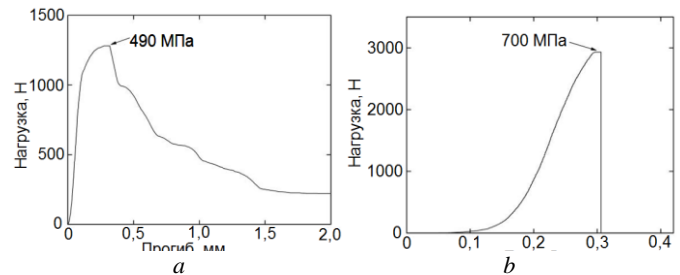


**Fig. 13.** Load-deflection curves of a composite made of layers of Nb-0.1% C alloy and layers of sapphire fibers in Nb-powder after DW (a) and after DW and HT (b)

Heat treatment at high temperatures, carried out after welding, significantly increased the ultimate strength of the composite, from 490 to 700 MPa. However, judging by the deformation curve, the material became significantly more brittle. The first thing that can explain such a degeneration of the material is the presence of aluminum in the composite and the formation of its intermetallic compounds with niobium.

Brittle compounds of aluminum with niobium Nb<sub>2</sub>Al and Nb<sub>3</sub>Al, formed during diffusion welding of the package at 1400°C, were also present in the samples after heat treatment at higher temperatures. Note that after HT at 1750°C and higher, only one intermetallic compound Nb<sub>3</sub>Al should remain. But after HT at 1950°C, the intermetallic precipitates of Nb<sub>3</sub>Al formed at lower temperatures could coagulate into larger ones, which would lead to the embrittlement of the entire composite. However, with such a sequence of transformations, a higher ultimate strength after DW + HT remains unexplained. It often happens that the coarsening of precipitates does not increase the strength of the material.

A slightly different development of the transformations seems more probable. After welding at 1400°C, a certain amount of intermetallic compounds was formed, which still does not negatively affect the fracture toughness of the material, but is also unable to provide the composite with a decent level of strength. The material after DW is plastic.

The next heat treatment of the composite at significantly higher temperatures caused the intensive formation of the intermetallic compound Nb<sub>3</sub>Al. As a result, the strength increased greatly, but the bending specimens showed a brittle state of the test material.

The deformation curves were used to determine the effective surface energy  $g$  of both composite materials, as the work of external forces applied to the sample, referred to the doubled area of its cross section [9]. In practice, it is determined by calculating the area under the experimental load-deflection curve. For the sample after DW (see Fig. 13, a), the value  $g = 9.2 \times 10^3$ , after DW + HT (see Fig. 13, b) –  $8.8 \times 10^3$  J/m<sup>2</sup>. The results are confirmed by microscopic observation data. After diffusion welding, the samples had a developed fracture surface (Fig. 14, a) with extended delamination. Subsequent heat treatment gave the structure proper intercomponent connectivity and completely eliminated delamination between the niobium-carbon alloy and sintered Nb powder (Fig. 14, b). However, the cohesive structure itself has less resistance to crack propagation. Therefore, both the sample deflection and the effective surface energy became smaller.

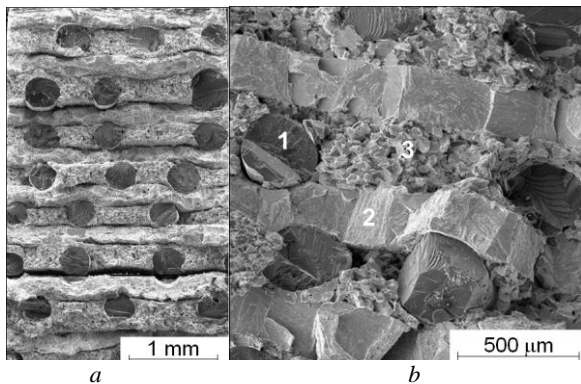


**Fig. 14.** Fracture surfaces of composites with a matrix based on Nb: after DW (a) and after DW + HT (b): 1 – fiber, 2 – Nb–0.1C foil layer, 3 – Nb-powder layer

The longitudinal structure of the composite (Fig. 15) was characterized by a regular arrangement of dense layers of cast alloy Nb–0.1C, porous layers of sintered Nb-powder and four sapphire fibers statistically found in the plane of the section. On top of the outer layer of the composite, you can see a thin layer of the heat-resistant coating we are developing.

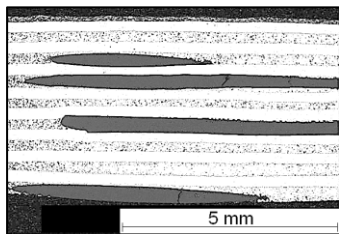


**Fig. 15.** Longitudinal sections of a composite after DW

In fig. 16 demonstrates the non-brittle nature of destruction of the laminated structure of the composite containing brittle fibers.

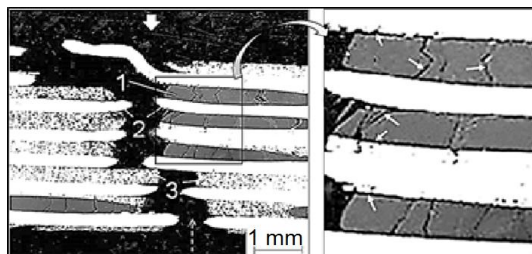


**Fig. 16.** Longitudinal sections of a composite after DW and after tests for strength: the arrow above shows the direction of load application; the dotted line is the direction of propagation of macrocracks: 1 – fiber, 2 – Nb–0.1C foil layer, 3 – layer of Nb-powder

Fragmentation of fibers 1 and delamination along the fiber-matrix boundaries (see arrows), plastic deformation with the formation of necks of the Nb–0.1C alloy 2, and nonplastic fracture of layer 3 with an inhomogeneous structure of Nb powder along grain boundaries are clearly visible. Microcracks in the fiber are retarded at the fiber-matrix boundaries. The fracture surface (see Fig. 14, a), formed after the passage of the macrocrack, confirms the described nature of the fractures.

The noted types of fractures, which are not in the plane of propagation of a macrocrack, increase the energy of inelastic scattering upon fracture of the composite and thereby increase the crack resistance of the material.

## 5. Summary and conclusions

1. Single crystal sapphire fibers obtained by the modified Stepanov method were used to reinforce a layered Nb-based composite developed for use at temperatures of 1300–1500°C. An

original procedure for testing fibers for bending is described. At a length of 10 mm, they had a strength exceeding 1000 MPa.

2. Developed and implemented in multilayer packages a hierarchically organized layered fibrous structure using foils of the Nb–0.1%C alloy, aluminum, Nb powder and sapphire fibers. The assembled package was subjected to diffusion pressure welding and subsequent heat treatment to obtain a composite with a layered-fiber structure reinforced with sapphire fibers.

3. The microstructure of the composites has been investigated. Strength bending tests have been carried out so far only at room temperature. The experimental load-deflection dependences made it possible to determine the effective surface energy of destruction of composites and to establish the correlation of mechanical characteristics with the structures of the composite after diffusion welding at 1400°C and after welding, followed by heat treatment at higher temperatures. The strength at room temperature exceeded 700 MPa, the effective surface energy was  $12 \times 10^5 \text{ J/m}^2$ .

4. The topography of the fracture surfaces of the composite specimens testified to the operation of various mechanisms of microfracture under loading of the material. Together, they provided the necessary fracture toughness to the composite containing brittle components.

5. The work and the results obtained are still more of a pilot nature, but will be the basis for further development and optimization of fiber composite structures, modes of their production using also other materials.

## Acknowledgments

The work was carried out within the of the Russian Academy of Sciences with partial funding from the Russian Foundation for Basic Research (project 20-03-00296).

## Literature

1. Properties, production and application of refractory compounds. Ed. Kosolapogo T.Ya. M.: Metallurgy, 1986, – 928 p.
2. Schneibel J.H. Intermetallics, 2003, No 11, pp. 625–632.
3. Sharif A.A., Misra A., Mitchell T.E. Scripta Materialia, 2005, No 52, pp. 399–402.
4. Jain P., Kumar K.S. Acta Materialia, 2010, v. 58, No 6, pp. 2124–2142.
5. A short guide to chemistry. Goronovsky I.T., Nazarenko Yu.P., Nekryach E.F. Kiev: Naukova Dumka, 1987, – 929 p.
6. Cook J., Gordon J.E. Proceedings of the Royal Society, 1964, v. 282, No 8, pp. 508.
7. Anischenkov V.M., Mileiko S.T. DAN SSSR, 1978, v. 241, No. 5, p. 1068.
8. Mileiko S.T. // Composite Science and Technology, 2001, v. 61, pp.1649–1652.
9. Ruditsin M.N., Artemov P.Ya., Lyuboshits M.I. A reference book on the strength of materials. Minsk: High. Sc., 1970. – 628 p.
10. Mileiko S.T. Comp. Sci. and Tech. // 2002, v. 62, p. 195–204.
11. Mileiko S.T., Kiiko V.M. // Mechanics of Composite Materials, 2004, vol. 40, p. 523–534.
12. Mechanics of a deformable solid. Yu.N. Rabotnov. Moscow: Nauka, 1979. –744 p.
13. Karpov M.I., Vnukov V.I., Stroganova T.S. et al. // Izvestia RAN. Physical series. 2019, vol. 83, no. 10, p. 1353–1361.
14. Svetlov I.L., Karpov M.I., Stroganova T.S., Zaitsev D.V., Artemenko Yu.V. Def. and destr. of mater., 2019, No. 11, p. 2–6.
15. Cook J., Gordon J.E. // Proceedings of the Royal Society A, 1964. – V. 282, Iss. 8. – P. 508–520.
16. Mileiko S.T. // Composites and nanostructures, 2015. – V. 7. No. 7. – P. 191–205.
17. Kurlov V.N., Stryukov D.O., Shikunova I.A. // Journal of Physics: Conference Series 673, 2016. – Art. 012017.
18. Kiiko V.M., Mileiko S.T. // Compos. Sci. Technol, 1999. – V. 59, Iss. 13. – P. 1977–1981.
19. Kurlov V.N., Shikunova I.A., Stryukov D.O. // RF Patent No. 2552436, Bulletin No. 16, 10.06.2015.